

The Pif1 signature motif of Pfh1 is necessary for both protein displacement and helicase unwinding activities, but is dispensable for strand-annealing activity

Jani B. Mohammad, Marcus Wallgren and Nasim Sabouri*

Department of Medical Biochemistry and Biophysics, Umeå University, SE-901 87, Umeå, Sweden

Received February 26, 2018; Revised July 08, 2018; Editorial Decision July 09, 2018; Accepted July 10, 2018

ABSTRACT

Pfh1, the sole member of the Pif1 helicases in *Schizosaccharomyces pombe*, is multifunctional and essential for maintenance of both the nuclear and mitochondrial genomes. However, we lack mechanistic insights into the functions of Pfh1 and its different motifs. This paper is specifically concerned with the importance of the Pif1 signature motif (SM), a 23 amino acids motif unique to Pif1 helicases, because a single amino acid substitution in this motif is associated with increased risk of breast cancer in humans and inviability in *S. pombe*. Here we show that the nuclear isoform of Pfh1 (nPfh1) unwound RNA/DNA hybrids more efficiently than DNA/DNA, suggesting that Pfh1 resolves RNA/DNA structures like R-loops *in vivo*. In addition, nPfh1 displaced proteins from DNA and possessed strand-annealing activity. The unwinding and protein displacement activities were dependent on the SM because nPfh1 without a large portion of this motif (nPfh1- Δ 21) or with the disease/inviability-linked mutation (nPfh1-L430P) lost these properties. Unexpectedly, both nPfh1-L430P and nPfh1- Δ 21 still displayed binding to G-quadruplex DNA and demonstrated strand-annealing activity. Misregulated strand annealing and binding of nPfh1-L430P without unwinding are perhaps the reasons that cells expressing this allele are inviable.

INTRODUCTION

Helicases are motor proteins driven by the energy from nucleoside triphosphate/deoxynucleoside triphosphate (NTP/dNTP) hydrolysis that unwind duplex nucleic acids, an activity that is crucial for numerous biological processes such as DNA replication, repair, transcription and trans-

lation. The Pif1 family of 5'-3' helicases belongs to the superfamily 1B (SF1B) helicases and contains helicases that are evolutionarily conserved from bacteria to humans (1,2). The number of Pif1 family members varies in different organisms, ranging from eight in *Trypanosoma brucei* to a single protein in humans and *Schizosaccharomyces pombe* (1).

Saccharomyces cerevisiae encodes two Pif1 helicases. These are the most extensively studied Pif1 helicases, and these studies have provided important information on the functions of the Pif1 family proteins (1). *Saccharomyces cerevisiae* Pif1 (ScPif1) and Rrm3 (ScRrm3) have both overlapping and nonoverlapping functions in the cell. An unanswered question is whether in organisms with a single Pif1 helicase member the helicase performs all or a mixture of the two ScPif1 helicase functions or if it resembles only one of them. ScPif1 is localized in both the nucleus and mitochondria, and it is needed during Okazaki fragment maturation and break-induced replication and is an inhibitor of telomerase (3–12). So far, ScRrm3 has known functions only in the nucleus, for example, promoting replication at 1400 genomic regions (13–16). These sites include, for example, DNA regions that are tightly bound by non-nucleosomal proteins at ribosomal DNA (rDNA), transfer RNA (tRNA) genes and the mating-type loci (3,13–15). There are two classes of impediments where fork progression is dependent on both ScPif1 and ScRrm3—R-loops at tRNA genes and predicted G-quadruplex (G4) structures (17–19).

Schizosaccharomyces pombe encodes only a single Pif1 family protein, named Pfh1 (20). Pfh1 is localized in both the nucleus and the mitochondria (21) where it is essential for the maintenance of both the nuclear and mitochondrial genomes (21), and immunoaffinity experiments combined with mass spectrometry have shown that Pfh1 interacts with both nuclear and mitochondrial proteins (22). Pfh1 promotes replication and suppresses DNA damage at hard-to-replicate genomic sites, including highly transcribed RNA polymerase II and III genes, replication fork

*To whom correspondence should be addressed. Tel: +46 90 786 50 00; Fax: +46 90 786 97 95; Email: nasim.sabouri@umu.se

barriers at rDNA and mating-type loci, telomeres, and predicted G4 structures (22–26). Although both ScRrm3 and Pfh1 bind preferentially to highly transcribed RNA polymerase II genes (22,23,27), only Pfh1 promotes replication at these sites (22,23). Pfh1, like ScRrm3, moves with the replisome (16,22) and, like ScPif1, is needed during Okazaki fragment maturation (8,9,28).

Mechanistic insights into how the eukaryotic Pif1 helicases perform their functions come mainly from ScPif1 because other eukaryotic Pif1 helicases are insoluble and/or unstable and are therefore difficult to purify. Recombinant ScPif1 is more processive on RNA/DNA hybrids than DNA/DNA substrates (29,30), unwinds G4 structures very efficiently (18,31,32), evicts protein from DNA (33–35) and possesses strand-annealing activity (36). The recombinant nuclear isoform of Pfh1 (nPfh1) binds and resolves G4 structures derived from G4 motifs from *S. pombe* telomeres and rDNA (37), two regions that are enriched in G4 motifs (25).

To date, only one disease-associated mutation in humans has been mapped to the Pif1 family helicases (38), and families with this mutation have increased risk of breast cancer (38). The mutation is located in the evolutionarily conserved Pif1 signature motif (SM), and the corresponding mutation in *S. pombe* leads to inviable cells (38). The SM exists only in Pif1 family helicases and is not found in other SF1B helicases (1). Therefore, some of the specific *in vivo* functions of the Pif1 family helicases might be connected to this motif. The SM encompasses 23 amino acid residues located between the conserved helicase motifs II and III. In our earlier analysis (1), we defined the SM as 21 amino acid residues; however, because the next two residues are also highly conserved in Pif1 helicases, we believe that 23 amino acid residues define the SM better. We also reported that the SM was missing in plants (1), but Pif1 helicases in plants are quite divergent, and Geronimo *et al.* have recently identified a less conserved SM in some plants (see accompanying paper by Geronimo *et al.* (39)).

There are four available crystal structures of Pif1 helicases (40), including the *Bacteroides* sp. 2-1-16 Pif1 (BaPif1) (41), *Bacteroides* sp. 3-1-23 Pif1 (42), human PIF1 (hPIF1) helicase domain (41) and *S. cerevisiae* truncated Pif1 (43). It is predicted that the leucine to proline mutation in the SM (hPIF1-L319P or the corresponding mutation) found in the families with increased risk of breast cancer introduces a kink in an α -helix leading to an impaired fold and loss of some or all protein functions (41).

To understand the mechanistic role of the SM, we performed side-by-side characterizations of the biochemical properties of nPfh1 and different nPfh1 SM variants. We expressed and purified an nPfh1 variant that lacked almost the entire SM (nPfh1- Δ 21), and several variants with point mutations at L430, which correspond to the mutation found in the families with increased risk of breast cancer. In this analysis, we discovered several new enzymatic activities of nPfh1 that might explain some of its *in vivo* functions, including a preference for unwinding RNA/DNA over DNA/DNA substrates, the ability to displace proteins from DNA and the ability to anneal complementary single-stranded nucleic acids. These data demonstrate that the Pif1 family helicases share a significant degree of conservation in biochemical

properties. Furthermore, we found that the SM was important for nucleic acid unwinding and protein displacement, activities that are ATPase-dependent. We also found that the SM is important for binding to some but not all nucleic acid substrates. However, the SM was dispensable for Pfh1's strand-annealing activity, and in the absence of adenosine triphosphate (ATP) nPfh1- Δ 21 displayed similar or even higher strand-annealing activity than nPfh1.

In summary, in addition to new insights into the enzymatic properties of nPfh1 and the SM, our findings also suggest that the inviability of *S. pombe* cells with the *pfh1-L430P* mutation and perhaps the increased risk of breast cancer in humans who carry this Pif1 variant might be caused not only by loss of Pfh1's/hPIF1's biochemical activities, but also by the binding of inactive Pfh1/hPIF1 to its target sites in a way that precludes the binding of a backup helicase. Our work on Pfh1's SM agrees well with data on ScPif1 in an accompanying paper, where they demonstrate that SM is needed for ScPif1's known biological functions that require ATPase hydrolysis (see accompanying paper by Geronimo *et al.* (39)).

MATERIALS AND METHODS

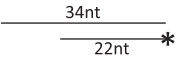
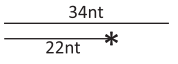
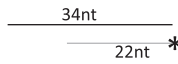
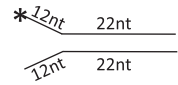

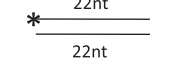
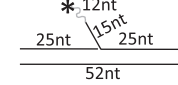
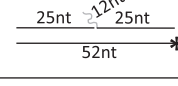
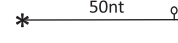
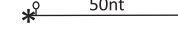
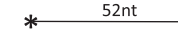
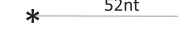

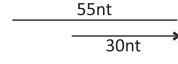
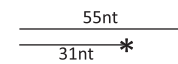
Preparation of the oligonucleotide substrates

To prepare the substrates (Table 1 and Supplementary Table S1), 1 μ l of 2.5 μ M single-stranded oligonucleotide was labeled at the 5' end with γ -³²P-ATP using 10 units of T4 polynucleotide kinase (ThermoFisher) and incubated at 37°C for 45 min in a total reaction volume of 20 μ l. The labeled oligonucleotides were subsequently purified on native polyacrylamide gel electrophoresis (PAGE) gels containing 1 \times Tris/Borate/EDTA (TBE) buffer. The radiolabeled oligonucleotides were mixed with cold complementary oligonucleotides at a 1:3 molar ratio in 25 μ l reactions containing 10 mM Tris-HCl (pH 7.5) and 50 mM NaCl. The reaction mixtures were then heated at 95°C for 5 min, slowly cooled down to room temperature, followed by purification on native PAGE gels. For the rDNA G4 DNA structure preparation, which forms an intermolecular G4 structure (37), 50 μ M of the rDNA G4 oligonucleotide from *S. pombe* (MWG-Biotech AG; see Supplementary Table S1) was heated at 95°C for 5 min in a buffer containing 10 mM Tris-HCl (pH 7.5) with 1 M NaCl, followed by slow cooling to room temperature (37). A total of 1 μ l of 5 μ M annealed G4 DNA was labeled at the 5' end with γ -³²P-ATP using the same conditions as above, followed by purification on native PAGE gels containing 1 \times TBE buffer and 10 mM NaCl.

Expression and purification of nPfh1

The expression and purification of the N- and C-terminally epitope-tagged nPfh1 and its mutated variants (His6-Trx-wild-type-FLAG (nPfh1), His6-Trx-K338A-FLAG (nPfh1-KA), His6-Trx-L430V-FLAG (nPfh1-L430V), His6-Trx-L430A-FLAG (nPfh1-L430A) and His6-Trx-nPfh1 Δ 21-FLAG (nPfh1- Δ 21); deleted region (⁴²⁸DKLEEVARVIRKDSKPFGGIQ⁴⁴⁸)) were performed as previously published for wild-type nPfh1 (37) with minor modifications. After transforming BL21(DE3)pLysS

Table 1. Substrates used in this study. * represents ^{32}P labeling; open circles represent biotin; the black dark lines are DNA; the gray straight or wavy lines are RNA; H is the helicase assay; E is the EMSA; PD is the protein displacement assay and SA is the strand-annealing assay

Name of the substrate	Structure	Type of assay
5'-3' DNA/DNA		H, E
3'-5' DNA/DNA		H, E
5'-3' RNA/DNA		H, E
Y-fork		H, E
rDNA G4		H, E
Duplex		H, E
Okazaki		H, E
Okazaki 12nt flap		H, E
3' Biotin		PD
5' Biotin		PD
ssDNA		E
ssRNA		E
ssRNA-DNA		E
5'-3' DNA/DNA		SA
3'-5' DNA/DNA		SA

competent cells with the plasmid, the cells were grown in Luria-Bertani (LB) media at 37°C until the OD₆₀₀ was ~0.6. The temperature was then reduced to 20°C, and protein expression was induced using 0.8 mM Isopropyl β-D-1-thiogalactopyranoside (IPTG). The cells were collected after 4 h, resuspended in lysis buffer (25 mM Tris-HCl (pH 7.5), 500 mM NaCl, 10 mM imidazole, 0.02% (v/v) Igepal, 5 mM β-mercaptoethanol, and 10% (v/v) glycerol) and stored at -80°C. Cell lysis was performed by sonication followed by centrifugation. The supernatant was mixed with 0.1 ml cComplete His-Tag Purification Resin (Roche) pre-equilibrated with lysis buffer and incubated under gentle rotation for 1 h at 4°C prior to loading onto a gravity flow column. Before elution, the column was washed with buffer B (25 mM Tris-HCl (pH 7.5), 500 mM NaCl, 30 mM imidazole, 0.02% (v/v) Igepal and 10% (v/v) glycerol). Elution of the target protein was performed with buffer B containing 300 mM imidazole, yielding five 1 ml fractions. Pure fractions were pooled and added to anti-FLAG M2 affinity resin, and 0.4 ml of FLAG buffer (25 mM Tris (pH 7.5), 500 mM NaCl, 0.02% (v/v) Igepal and 10% (v/v) glycerol) containing 0.2 mg/ml FLAG peptide (Sigma-Aldrich) was added to the column and incubated for 30 min at 4°C before collecting the eluate. This elution procedure was repeated two times. Finally, to eliminate the co-eluted FLAG peptide, the pure fractions were pooled together and loaded onto a PD10 column (GE Healthcare). The eluted protein was concentrated using an Amicon filter unit (Millipore) with a molecular weight cut-off of 30 kDa followed by flash-freezing in liquid nitrogen before storage at -80°C. Protein purity was assessed by sodium dodecyl sulphate-polyacrylamide gel electrophoresis (SDS-PAGE), and the protein concentration of nPfh1 was determined by Bradford assay (Roche Life Science). The concentration of nPfh1 was then used as a reference to determine the concentrations of all other nPfh1 variants by quantifying the nPfh1 and nPfh1 variant from SDS-PAGE protein bands (the same volume loaded for each protein variant) using ImageJ.

Due to low expression levels of soluble protein, the expression procedure was slightly changed for His6-Trx-L430P-FLAG (nPfh1-L430P) and His6-Trx-Δ21-FLAG (nPfh1-Δ21). The transformed cells were grown to an OD₆₀₀ ~0.6 at 37°C followed by induction of protein expression with 0.1 mM IPTG and continued cell growth at 15°C for 18–20 h.

Electrophoretic mobility shift assay (EMSA) and helicase assay

The DNA binding reactions were performed in 20 μl reaction mixtures containing 50 mM Tris-HCl (pH 8.5), 2 mM Dithiothreitol (DTT), 0.25 mg/ml bovine serum albumin (BSA), 2 mM MgCl₂, 100 mM NaCl, and 4 fmol ^{32}P -labeled DNA (final concentration of 0.2 nM). The reaction was started by addition of protein (final concentrations of 9.6, 96 pM, 0.96 or 9.6 nM for nPfh1 and nPfh1-KA and 0.96 or 9.6 nM for the other mutants) and incubated for 10 min at 30°C. The samples were subjected to electrophoresis using a 10% native polyacrylamide gel in 1× TBE buffer in the gel and the running buffer (for the G4 substrate, 10 mM

NaCl was added in the gel and buffer). The gel was dried, exposed to a phosphorimager screen (Fujifilm) overnight and visualized with a Typhoon 9400 Variable Mode Imager (Amersham Biosciences/GE Healthcare).

The procedure to determine the helicase activity of the nPfh1 protein variants was similar to the electrophoretic mobility shift assay (EMSA), with the exception of adding ATP to the reaction mixture. After 10 min incubation at 30°C, the reaction was stopped by adding 4 μ l of 6 \times stop solution (60 mM ethylenediaminetetraacetic acid (EDTA) (pH 8.0), 40% (w/v) sucrose, 0.6% SDS, 0.25% bromophenol blue, 20 nM unlabeled oligonucleotide and 0.5 mg/ml proteinase K) on ice. To separate intact DNA from unwound product, electrophoresis was performed using a 10% native polyacrylamide gel in 1 \times TBE buffer (with 10 mM NaCl in both the gel and running buffer for the G4 substrate). For both the EMSA and helicase assay, the gel bands were quantified with the ImageQuant software. To calculate the amount of bound or unwound DNA, the formula [% bound or unwound = 100 \times (P/(P + S))] was used, where P is unwound or bound DNA and S is the background-corrected (no protein added) unbound or intact DNA.

Streptavidin displacement assay

The streptavidin displacement assay (44) was carried out in 20 μ l of reaction mixtures containing 50 mM Tris-HCl (pH 8.5), 2 mM DTT, 0.25 mg/ml BSA, 2 mM ATP, 2 mM MgCl₂, 100 mM NaCl, and 4 fmol (final concentration of 0.2 nM) ³²P-labeled 3' biotin-coupled or 5' biotin-coupled poly(T)₅₀ oligonucleotides. Streptavidin (1 μ M) was added to the reaction mixtures followed by incubation for 5 min on ice to enable binding of streptavidin to the biotin moiety. The displacement reaction was then initiated by adding various concentrations of nPfh1 (final concentrations of 1, 4, 10 or 25 nM for nPfh1 and nPfh1-KA; 10 or 25 nM for the other mutants) together with 100 μ M biotin as a trap for dissociated streptavidin. The reaction was incubated for 10 min at 30°C and stopped by adding 10 μ l of 3 \times stop solution (75 mM EDTA (pH 8.0), 10% (v/v) glycerol, 3% SDS, 0.3% bromophenol blue and 3 mg/ml proteinase K) followed by incubation for 15 min at 37°C. The samples were subjected to electrophoresis on a 10% native polyacrylamide gel. To calculate the amount of displaced streptavidin, the formula [% Displacement = 100 \times (P/(P + S))] was used, where P is the amount of streptavidin-displaced DNA and S is the amount of background-corrected (no protein added) streptavidin-bound DNA.

Strand-annealing assay

To determine the strand-annealing capacity of nPfh1, we used 20 μ l of reaction mixtures containing 50 mM Tris-HCl (pH 8.5), 2 mM DTT, 0.25 mg/ml BSA, 2 mM MgCl₂, 100 mM NaCl, and 4 fmol ³²P-labeled DNA (final concentration of 0.2 nM). Each substrate was tested in the presence and absence of 2 mM ATP. The strand-annealing reaction was started by adding various concentrations of nPfh1 (final concentration of 9.6, 96 pM, 0.96 or 9.6 nM for wild-type nPfh1 and nPfh1-K338A; 0.96 or 9.6 nM for the other

variants) and incubated for 10 min at 30°C. The reactions were stopped by adding 10 μ l of 3 \times stop solution (75 mM EDTA (pH 8.0), 10% (v/v) glycerol, 3% SDS, 0.3% bromophenol blue, 100 nM unlabeled oligonucleotide and 3 mg/ml proteinase K), followed by incubation for 15 min at 37°C. The samples were subjected to electrophoresis using a 10% native polyacrylamide gel. To calculate the amount of annealed DNA, the formula [% annealed product = 100 \times (P/(P + S))] was used, where P is the amount of annealed DNA and S is the amount of background-corrected (no protein added) single-stranded DNA.

ATPase assay

The ATPase assay was carried out using 6 nM nPfh1 and incubated for 20 min at 30°C in the presence of 100 nM 52 nt single-stranded DNA in a buffer containing 50 mM Tris-HCl (pH 8.5), 100 mM NaCl, 5 mM MgCl₂, 2 mM DTT and 2 mM ATP in a reaction volume of 50 μ l. A total volume of 100 μ l of BIOMOL Green reagent (Enzo Life Sciences) was added to the reaction followed by a 25 min incubation at room temperature before measuring the absorbance at 620 nm using an Infinite M200 plate reader (TECAN). The measurements were performed with the following parameters: 3 s shaking (2 mm amplitude, orbital mode, 57 rpm frequency), 25 flashes and 0 ms settle time. The amount of phosphate released was calculated using the phosphate standard provided in the kit (Enzo Life Sciences) according to the manufacturer's instructions.

Far-UV circular dichroism (CD) spectroscopy

The secondary structures of the wild-type nPfh1, nPfh1-L430V and nPfh1-L430A proteins were analyzed using a JASCO J-710 Spectropolarimeter (JASCO) equipped with a Peltier element for temperature control. To perform the circular dichroism (CD) measurements, 1 μ M (nPfh1 and nPfh1-L430V) or 0.5 μ M (nPfh1-L430A) protein was put into a 1 mm path length quartz cuvette (Hellma), and spectra were collected from 200 to 260 nm at 30°C using the following parameters: 0.5 nm data pitch, continuous, 50 nm/min scanning speed, 1 s response, 2 nm bandwidth, 8 spectra accumulations and 100 millidegrees standard sensitivity. The background from the buffer was corrected using a sample containing no protein.

RESULTS

nPfh1 unwinds RNA/DNA substrates more efficiently than DNA/DNA substrates

To determine the unwinding substrate specificity of nPfh1, we performed helicase assays. For all described assays, we used ³²P 5'-end-labeled oligonucleotides (Table 1). In all helicase assays, the reactions were started by adding different concentrations of nPfh1 or helicase-inactive nPfh1-KA. nPfh1-KA carries a mutation located in the invariant K of the Walker A box, and this mutation eliminates ATPase activity in all tested helicases. For both nPfh1-KA and wild-type nPfh1, we tested protein concentrations from 9.6 pM to 9.6 nM. As expected, nPfh1-KA did not unwind any of

the tested substrates, even at the highest protein concentration, and this confirmed that the unwinding properties that we detected in the nPfh1 reactions were due to nPfh1 and not to any helicase contaminants in the protein preparation.

We first confirmed that nPfh1 unwinds an rDNA G4 structure very efficiently because at 96 pM the unwinding activity was already saturated (Figure 1). Thus, our current recombinant nPfh1 behaved similarly to our previously purified protein (37). Because ScPif1 unwinds an RNA/DNA partial duplex substrate more efficiently than a DNA/DNA partial duplex substrate (29,30), we determined whether nPfh1 has similar properties. For these experiments, we annealed 0.2 nM of a 22 nt RNA oligonucleotide to a 34 nt DNA oligonucleotide, where 22 nt of the DNA oligonucleotide was complementary to the RNA oligonucleotide. Thus, the substrate had a 12 nt 5' single-stranded overhang (Table 1). Even at 96 pM of nPfh1, 26% of the RNA/DNA partial duplex substrate was unwound, and unwinding was saturated at 0.96 nM (Figure 1). In side-by-side reactions, we compared the activity of nPfh1 unwinding of the RNA/DNA substrate to a DNA/DNA substrate in which a 22 nt DNA oligonucleotide was annealed to the same 34 nt DNA oligonucleotide. At 96 pM, only 6% of the DNA/DNA partial duplex substrate was unwound, showing that nPfh1 unwound an RNA/DNA substrate more efficiently than a similar DNA/DNA substrate (Figure 1). These results show that nPfh1 efficiently removes an RNA oligonucleotide annealed to a DNA oligonucleotide, suggesting that nPfh1 might remove R-loops or other RNA/DNA substrates *in vivo*. We also determined if nPfh1 can unwind a DNA/DNA partial substrate with a 3' single-stranded overhang or a duplex DNA substrate without a flap, but nPfh1 was unable to unwind these substrates (Supplementary Figure S1). Thus, our recombinant nPfh1 only had 5'-3' activity and needed an oligonucleotide flap for unwinding.

Replication fork structures are unwound by nPfh1

To confirm previous observations from the Seo lab that a different recombinant Pfh1 (NusA-Pfh1) unwinds substrates resembling a Y-fork and an Okazaki fragment (28), we also examined if our nPfh1 can unwind these substrates. We prepared a Y-fork substrate with a 22 nt duplex region with both 5' and 3' 12 nt single-stranded overhangs (Table 1). nPfh1 unwound the Y-fork and showed a higher unwinding activity of the Y-fork substrate compared to the partial DNA/DNA duplex with only a 5' single-stranded tail, indicating that a forked structure stimulates the unwinding activity of nPfh1 more than the partial DNA/DNA duplex substrate (Figure 1). Thus, as with ScPif1 (11,35) and NusA-Pfh1 (28), nPfh1 was more active on a forked DNA structure than on the partial DNA/DNA duplex substrate (Figure 1).

Next, we determined if nPfh1 can unwind a substrate that resembles an Okazaki fragment with a 27 nt single-stranded RNA–DNA chimeric flap. The 27 nt flap consisted of 12 nt RNA on the 5' end plus 15 nt DNA (Table 1) (28). nPfh1 removed the RNA–DNA chimeric oligonucleotide very efficiently (Figure 1), which suggests that nPfh1 might be able to remove RNA–DNA flaps during

Okazaki fragment maturation and agrees with earlier observations made with NusA-Pfh1 recombinant protein (28). nPfh1 unwound the Okazaki fragment substrate more efficiently than the Y-fork substrate (Figure 1); however, the Y-fork substrate contained 12 nt single-stranded flaps, while the Okazaki fragment substrate had a longer 27 nt single-stranded flap. To determine if the efficient unwinding of the Okazaki substrate was due to the longer flap, we used another Okazaki substrate that contained a 12 nt single-stranded RNA flap, which was the same length as the Y-fork flaps (Table 1). nPfh1 was able to unwind this substrate as well (Supplementary Figure S2); however, the unwinding efficiency was strongly reduced compared to the Okazaki fragment with the longer 27 nt flap (38% compared to 83% at 9.6 nM protein), suggesting that the length of the flap affects the unwinding efficiency of nPfh1 and that single-stranded RNA on the flap does not hinder unwinding by nPfh1. Together, our helicase assays indicate that nPfh1 unwinds the tested substrates with different efficiencies: rDNA G4 (77%) > Okazaki fragment substrate with a 27 nt flap (69%) > Y-fork (41%) > RNA/DNA partial duplex (27%) > DNA/DNA partial duplex (6%) > Okazaki fragment substrate with a 12 nt flap (<5%), where the numbers in parentheses indicate the percentage of unwound DNA by 96 pM nPfh1 (Figure 1B).

The substrate binding preference of nPfh1 is similar to its substrate unwinding preference

A possible explanation for the hierarchy of efficiency of unwinding of the tested substrates is that the binding affinity of nPfh1 varies between different substrates. To test this possibility, we performed EMSA experiments with the same substrates that were used in the helicase assays. To prevent nPfh1 from unwinding the substrates, ATP was excluded from the reactions. Similar to the helicase assays, we incubated 0.2 nM of substrate with different concentrations of nPfh1 or nPfh1-KA (9.6 pM to 9.6 nM). The binding preference for nPfh1-KA was similar to nPfh1 for all tested substrates (Figure 2). As previously observed, nPfh1 bound to rDNA G4 as indicated by the induced shift in mobility of the substrate (Figure 2A). The shift was detected even at 96 pM nPfh1, and at 9.6 nM all of the DNA was shifted. These results confirmed our previously published data showing that nPfh1 binds the rDNA G4 structure (Figure 2A) (37).

We observed very faint DNA shifts with both the 5'-3' DNA/DNA and RNA/DNA partial duplexes, even at a ~50-fold excess of protein to DNA (lane 5 in the DNA/DNA and RNA/DNA gel images in Figure 2A). These results suggest that binding of nPfh1 to both of these substrates is weak (Figure 2A). We did not detect binding to the 3'-5' partial duplex or to the duplex substrates (Supplementary Figure S3). The extent of nPfh1 binding (9.6 nM nPfh1) to the Y-fork substrate was ~6-fold higher than to the 5'-3' partial duplex substrates (20% versus 3% binding) (Figure 2A).

The unwinding of the Okazaki fragment with the long flap by nPfh1 was more efficient than observed for the Y-fork substrate, but less efficient than for the rDNA G4 substrate (Figure 1). This hierarchy was also reflected in the binding efficiency, and nPfh1 induced a shift at about a 5-

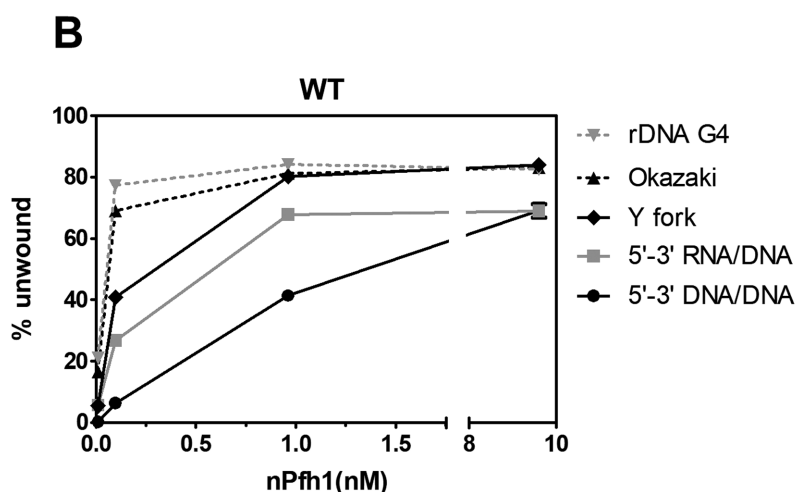
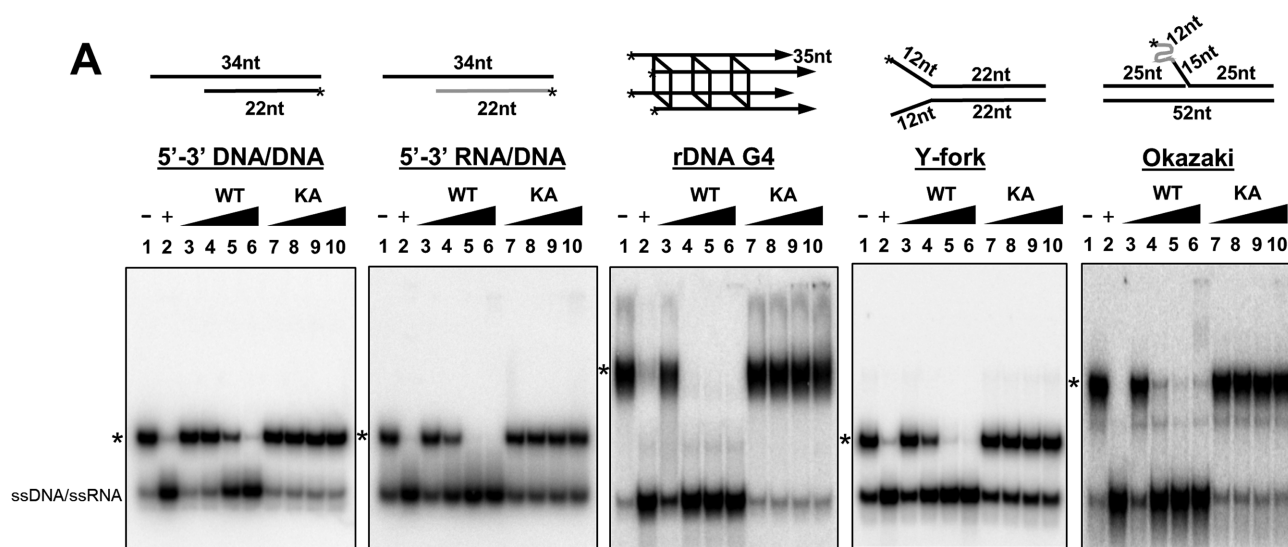


Figure 1. nPfh1 unwinds G4 DNA, RNA/DNA substrates and replication fork structures. (A) Helicase assays were performed with various substrates, including a partial DNA duplex (5'-3' DNA/DNA), a partial RNA/DNA duplex (5'-3' RNA/DNA), intermolecular G4 DNA (rDNA G4), a fork-like Y-structure (Y-fork) and an Okazaki RNA–DNA chimeric substrate with a longer flap (Okazaki). The position of each annealed/folded substrate on the gel is indicated with an asterisk. We incubated 0.2 nM 32 P-labeled substrate for 10 min with 9.6, 96 pM, 0.96 or 9.6 nM nPfh1 (WT) or nPfh1-K338A (KA) and separated the reaction products on 10% native polyacrylamide gels. Lanes 1 and 2 are with DNA in the absence of protein. The substrate in lane 1 was unboiled (–), and the substrate in lane 2 was boiled (+) being loaded on the gel. (B) Graph showing quantification of the unwound substrates. Each experiment was repeated three times, and the mean percentage of unwound product was calculated. Here and hereafter, error bars represent standard deviations.

fold excess of protein to DNA, which was a lower protein concentration than that needed to shift the Y-fork substrate but higher than that needed to shift the rDNA G4 substrate (Figure 2A). Together these experiments suggest that the binding efficiency to the substrates examined by EMSA corresponds well to the unwinding efficiency of the substrates by nPfh1. The only exception was the partial duplex RNA/DNA and DNA/DNA substrates, where very weak binding was detected by EMSA for both substrates, yet the unwinding efficiency was higher for the RNA/DNA partial duplex compared to the DNA/DNA partial duplex substrate (Figures 1 and 2). Given that the two substrates were

bound with similar affinities, the data suggest that nPfh1 displaces an RNA oligonucleotide more efficiently than a DNA oligonucleotide.

To determine if the differences in the binding efficiencies of nPfh1 were due to the chemical identity of the nucleic acid (i.e. RNA versus DNA), we examined binding of nPfh1 to 52 nt substrates of single-stranded DNA or single-stranded RNA, as well as to the single-stranded RNA–DNA chimeric oligonucleotide. nPfh1 bound similarly to the single-stranded DNA and single-stranded RNA oligonucleotides, and had slightly reduced binding to the single-stranded RNA–DNA chimeric oligonucleotide (Fig-

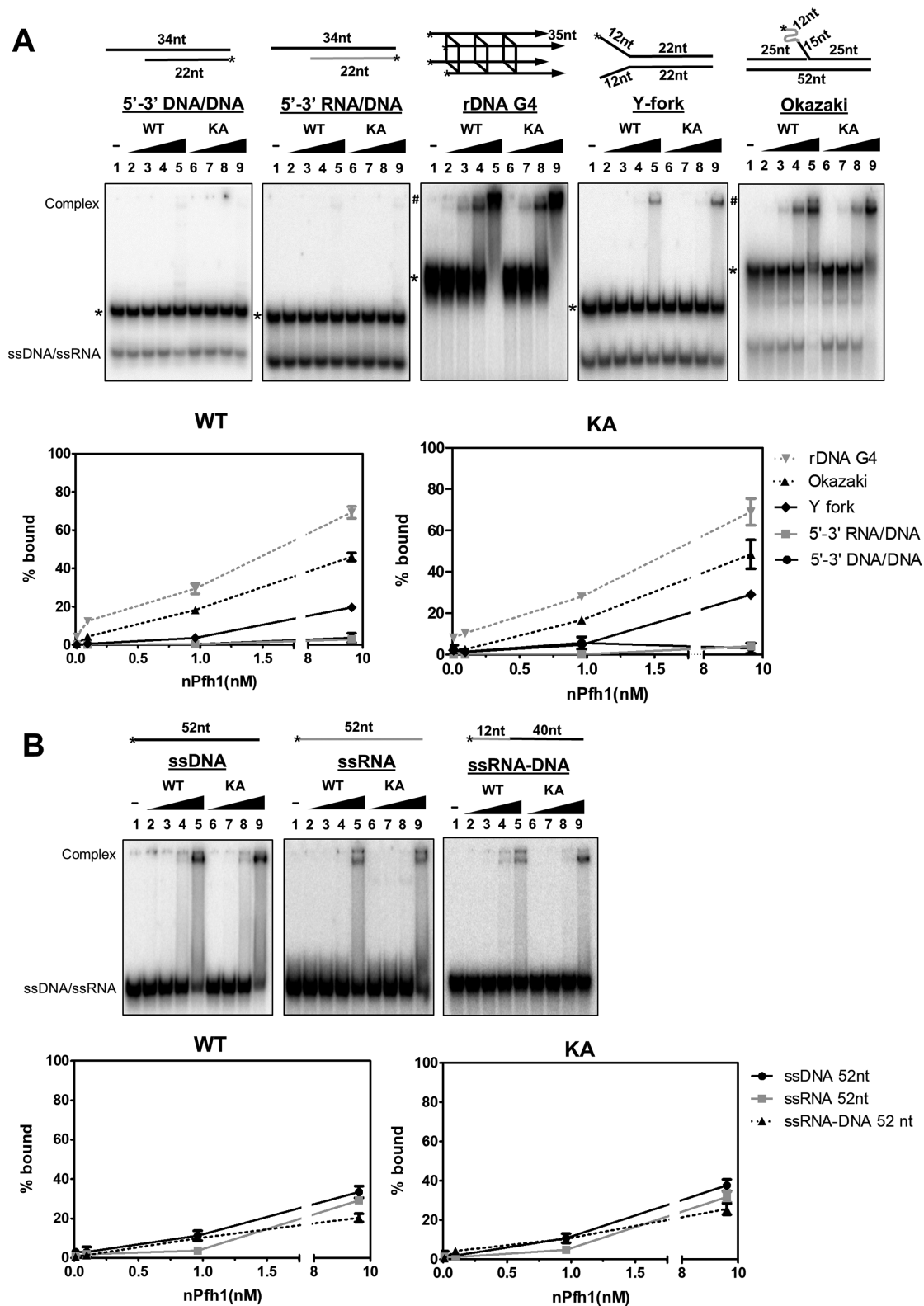


Figure 2. G4 DNA and Okazaki fragments are efficiently bound by nPfh1. (A) (Top) EMSA was performed on different substrates using 0.2 nM ^{32}P -labeled oligonucleotides. The same substrates as in Figure 1 were used, and the position of each annealed/folded substrate on the gel is indicated with an asterisk. # indicates protein/DNA in the wells of the rDNA G4 and Okazaki substrates. Each substrate was treated with 9.6, 96 pM, 0.96 or 9.6 nM WT or KA and analyzed on 10% native polyacrylamide gels. Lane 1 on each gel is labeled '-' and shows DNA in the absence of protein. (Bottom) For each DNA substrate, the amount of protein bound to DNA was determined from the bands labeled 'complex' in the EMSA gels at the top, and the mean percentage of bound protein from three independent experiments is shown. (B) (Top) EMSA was run on single-stranded (ss) DNA, RNA and RNA-DNA and analyzed as in (A). (Bottom) Quantification of the percentage of bound protein to single-stranded DNA/RNA was performed as in (A).

ure 2B). We suggest that the differences in Pfh1 binding to different substrates may be dictated by structures, and probably not chemical identity, because nPfh1 does not discriminate between the tested single-stranded DNA and single-stranded RNA oligonucleotides.

nPfh1 removes streptavidin from single-stranded DNA

Pfh1, ScRrm3 and ScPif1 have all been suggested to remove proteins from the DNA. To determine if nPfh1 can evict proteins from DNA, we set up a protein displacement assay. We incubated 0.2 nM biotin labeled single-stranded DNA with streptavidin, which strongly binds biotin. To determine if nPfh1 removes streptavidin from DNA, we incubated the reaction with different amounts of nPfh1 or nPfh1-KA (1–25 nM) and separated the reaction products on a native polyacrylamide gel. If streptavidin was displaced, a faster migrating band should be detected.

First, as a control, only biotin was added without any helicase and was compared to a reaction without addition of biotin (Figure 3A, lanes 1 and 2). In these reactions, we detected a slight increase of the faster migrating band, suggesting that some of the streptavidin molecules were displaced when adding an excess amount of free biotin to the reaction (Figure 3A, lanes 1 and 2). Next, we added increasing amounts of nPfh1 to the reaction, which resulted in increased amounts of the faster migrating band in the gel (Figure 3A, lanes 3–6), indicating that nPfh1 removed streptavidin from DNA and suggests that nPfh1 has the ability to remove proteins from DNA. We did not detect any significant streptavidin displacement when the biotin was positioned on the 5' end of the oligonucleotide (Supplementary Figure S4, lanes 3–6), demonstrating that nPfh1 can only remove streptavidin when translocating in the 5'-3' direction. nPfh1-KA was unable to remove streptavidin from either of the 5' or 3' biotinylated templates (Figure 3A, lanes 7–10 and Supplementary Figure S4, lanes 7–10), showing that the ATPase activity is needed for this function.

Complementary DNA strands are annealed by nPfh1 and nPfh1-KA

Some helicases not only have an unwinding property, but can also rewind two complementary strands of nucleic acids (45). For example, both hPIF1 and ScPif1 can rewind two complementary DNA strands in an ATP-independent manner (36,46). To determine if nPfh1 has similar strand-annealing activity, we first mixed 0.2 nM of the two single-stranded complementary substrates from a partial duplex DNA/DNA substrate (Table 1) to determine if the oligonucleotides could anneal spontaneously. We detected very small amounts of a band that corresponded to the size of the annealed product, suggesting that the oligonucleotides can spontaneously anneal only to a very low extent in the absence of helicase (Figure 3B, lane 1). To promote annealing, we heated the oligonucleotides to 95°C and slowly cooled them. As expected, the two complementary oligonucleotides annealed efficiently (Figure 3B, lane 2). To test if nPfh1 possesses strand-annealing activity, we mixed the two complementary oligonucleotides and added increasing amounts of nPfh1 to the reaction (9.6 pM to 9.6 nM). The

reaction was carried out in the absence of ATP to eliminate the helicase activity of nPfh1. nPfh1 promoted annealing of the two complementary oligonucleotides, and at 9.6 nM nPfh1 ~19% of the oligonucleotides were annealed (Figure 3B and C). To confirm that the ATPase activity was unnecessary for nPfh1-promoted annealing, we performed the same experiment with nPfh1-KA (Figure 3B). Because nPfh1-KA and nPfh1 annealed the oligonucleotides with the same efficiency, hydrolysis of ATP is not necessary for nPfh1's strand-annealing activity (Figure 3B and C).

To determine the need for ATP in the nPfh1-mediated annealing in more detail, we performed additional strand-annealing assays where we either excluded or included ATP. To prevent nPfh1 from unwinding the annealed product, we used oligonucleotides from a 3'-5' partial duplex substrate (Table 1). First, we determined if nPfh1 and nPfh1-KA could anneal the complementary oligonucleotides from the 3'-5' partial duplex substrate in the absence of ATP. Both nPfh1 and nPfh1-KA annealed the two complementary oligonucleotides (Figure 3B and C), however less efficiently than with the 5'-3' partial duplex substrate, suggesting that nPfh1 is more efficient in annealing a substrate with a 5' tail compared to a 3' tail. To determine the effect of ATP, we repeated the same experiment but included ATP. The presence of ATP significantly ($P < 0.002$) increased the amount of annealed 3'-5' partial duplex product in the presence of nPfh1 (10–21%), but not in the presence of nPfh1-KA (11–7%). These findings demonstrate that while nPfh1 does not require ATP for strand annealing, ATP hydrolysis significantly enhances the strand-annealing properties of nPfh1 (Figure 3B and C).

nPfh1 with a leucine to valine substitution in the SM retains both helicase and ATPase activity

The SM consists of a 23 amino acid region that is unique to Pif1 family helicases (Figure 4A) (1,47–49). We generated a mutant in which the first 21 amino acids of the SM were deleted (nPfh1- Δ 21) (Figure 4A). Because the corresponding L430P mutation in this motif is associated with increased risk of breast cancer, we also generated three mutations of this residue, nPfh1-L430A, nPfh1-L430V and nPfh1-L430P (Figure 4A). Each variant was expressed in *Escherichia coli* and purified (Figure 4B).

We first examined the ability of the SM variants to unwind different substrates using our standard helicase conditions but using only helicase concentrations of 0.96 and 9.6 nM. nPfh1-L430V was the most active of the mutant proteins and was able to unwind all of the tested substrates, albeit to different extents and in each case to a lesser extent than nPfh1. For example, at 0.96 nM, nPfh1-L430V unwound ~58% of the rDNA G4 substrate, while nPfh1 unwound ~84% (Figures 1 and 4C and D). Together, this suggests that nPfh1-L430V still possesses some of the nPfh1 properties, but not to the same extent as wild-type protein. The other mutated variants displayed no or only very weak unwinding activity at both concentrations and on all substrates (Figure 4C and D).

Next, we asked if a loss of ATPase activity explained the reduction or absence of helicase activity in the SM variants. Although the ATPase activity of nPfh1-L430V was similar

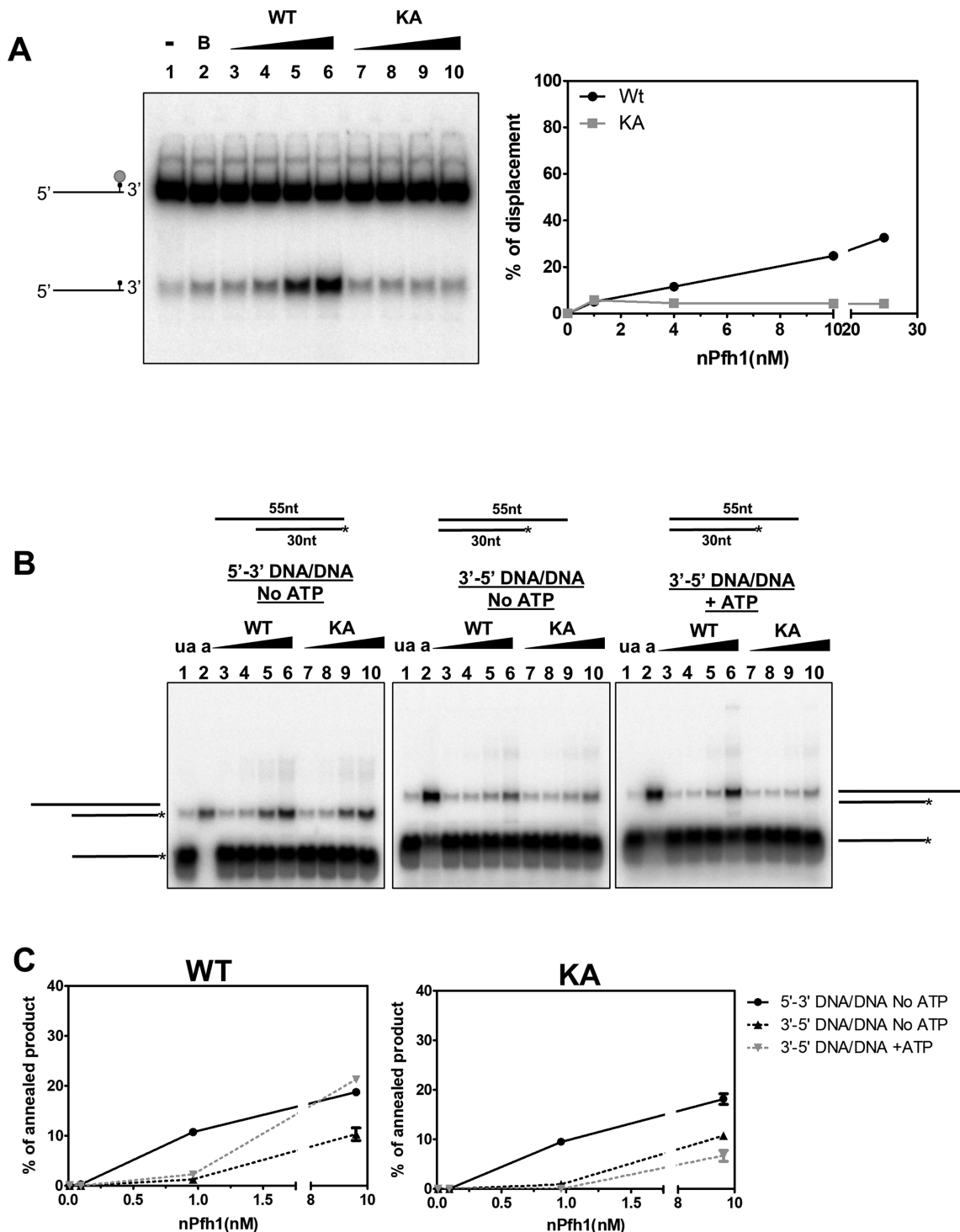


Figure 3. nPfh1 displaces protein from DNA and exhibits strand-annealing activity. (A) (Left image) A streptavidin displacement assay using biotin conjugated to the 3' end of the DNA was performed. ^{32}P -labeled biotinylated oligonucleotide (0.2 nM) was incubated with streptavidin and different concentrations (1, 4, 10 and 25 nM) of WT (lanes 3–6) or KA (lanes 7–10). The reaction was started by addition of the helicase and free biotin, run for 10 min at 30°C and analyzed on 10% native polyacrylamide gels. ‘–’ indicates no helicase or biotin added (lane 1), and ‘B’ indicates that biotin was added as a control, but no helicase (lane 2). The cartoon on the left side of the gel shows a biotinylated oligonucleotide with or without a streptavidin molecule (filled gray circle). (Right image) Graph showing the mean percentage of protein displacement from three independent experiments. (B) The strand-annealing assays were conducted using 0.2 nM of a ^{32}P -labeled 30 nt single-stranded DNA (5'-3' DNA/DNA substrate) or a 31 nt DNA oligonucleotide (3'-5' DNA/DNA substrate) in the absence (no ATP) or presence of ATP (+ATP). The reactions were started by incubating the single-stranded labeled DNA oligonucleotide together with different amounts of nPfh1 (WT) or nPfh1-K338A (KA) and the corresponding complementary cold DNA template (55 nt). In lane 1, in all gels, both the labeled oligonucleotide and the cold oligonucleotide were added without the helicase and incubated at 30°C for 10 min (ua: unannealed). Lane 2 shows the positive control for an annealed product (a: annealed). (C) Graphs showing the mean proportion of annealed product for WT (left) or KA (right) for the gels in (B). Each experiment was repeated three times.

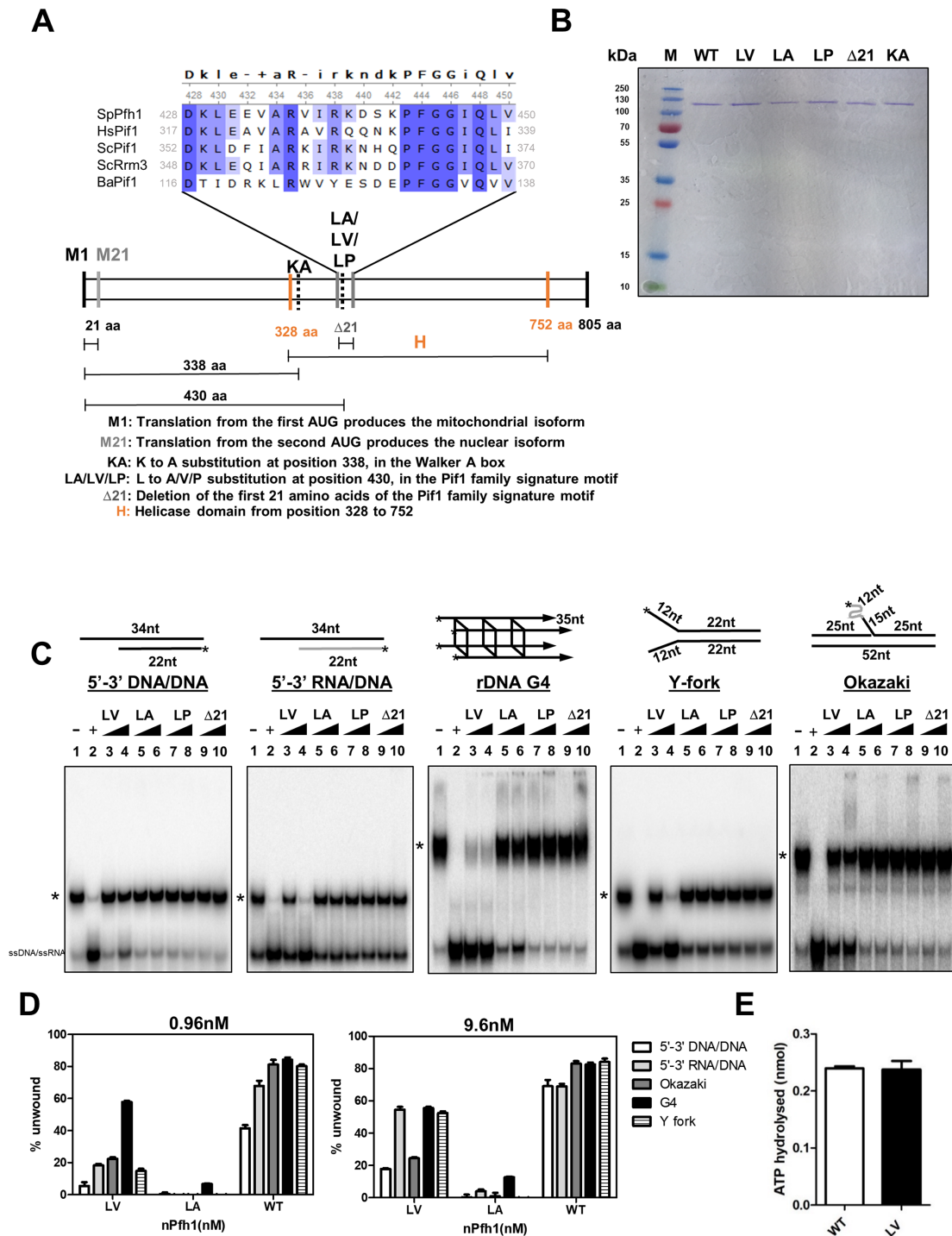


Figure 4. The SM is indispensable for DNA unwinding. (A) Schematic of the whole *pfh1*⁺ gene and sequence alignment of the 23 amino acid residues of SM. The sequence of the SM was aligned from the following organisms using CustalW (47): *Schizosaccharomyces pombe* (Sp), *Homo sapiens* (Hs), *Saccharomyces cerevisiae* (Sc) and *Bacteroides* sp. 2-1-16 (Ba). Protein sequences were downloaded from PomBase (*S. pombe*) (48) and NCBI. The alignment was analyzed using Unipro UGENE (49). The numbering on the top and on the sides shows the position of the *S. pombe* and the other organisms' amino acid residues, respectively. The consensus sequence is shown above the alignment. '+' indicates two or more residues are equally abundant, and '-' indicates no conserved residues. The amino acids are highlighted in dark blue (conserved), blue (identical between four organisms) or light blue (identical between three organisms). (B) Coomassie blue staining of purified nPfh1 (WT), nPfh1-L430V (LV), nPfh1-L430A (LA), nPfh1-L430P (LP), nPfh1 with deletion of 21 amino acids of SM (Δ 21) and helicase-inactive nPfh1-K338A (KA). (C) Helicase assays were performed with the different nPfh1 variants (LV, LA, LP or Δ 21) described in (A) using the same substrates as in Figure 1. The reactions were incubated with either 0.96 or 9.6 nM of the nPfh1 variants. '*' denotes the position of the folded/annealed substrate. (D) The mean percentage of unwound product by LV and LA from the gels in (C) was calculated from three independent experiments. Quantification data for wild-type nPfh1 are from Figure 1. (E) The mean amount of ATP hydrolysed at 30°C by 6 nM WT and LV after 20 min incubation in the presence of 100 nM single-stranded 52 nt DNA oligonucleotide from three experiments. The error bars represent standard deviations.

to that of nPfh1, the other nPfh1 variants were inactive in this assay (Figure 4E and data not shown). These findings suggest that the low helicase activity of all but the nPfh1-L430V mutant can be explained by low ATPase activity and that the reduced helicase activity of nPfh1-L430V must be due to something other than impaired ATP hydrolysis.

nPfh1-L430P and nPfh1-Δ21 bind to G4 DNA and Okazaki fragment-like substrates

To determine if reduced ATPase or helicase activity was due to reduced substrate binding, we tested the SM variants for binding efficiency to different substrates. We performed EMSA with either 0.96 or 9.6 nM of each variant using the same conditions described above. Similar to nPfh1 and nPfh1-KA, the SM variants had no or only very weak binding to the short-flap Okazaki fragment substrate as well as to both the RNA/DNA and DNA/DNA partial duplex substrates (Figure 5A and Supplementary Figure S5). nPfh1-L430V showed slightly weaker binding to the Y-fork substrate than nPfh1 (13% and 20%, respectively), while nPfh1-L430A, nPfh1-L430P and nPfh1-Δ21 showed less than 5% binding to this substrate. Unexpectedly, all of the nPfh1 SM variants bound the rDNA G4 to almost the same extent or slightly better than the wild-type nPfh1 (~40–80% binding for the nPfh1 variants compared to 70% for wild-type nPfh1). In addition, all variants except nPfh1-L430A bound the long-flap Okazaki fragment substrate almost as efficiently as wild-type nPfh1 (Figure 5A). However, when nPfh1-L430A, nPfh1-L430P and nPfh1-Δ21 bound these substrates, the formed DNA–protein complex did not migrate into the gel as for wild-type nPfh1 and nPfh1-L430V (Figures 2A and 5A).

We also used EMSA to determine if the nPfh1 variants still bound to single-stranded DNA or RNA–DNA oligonucleotides. The nPfh1 variants, except nPfh1-L430V, had no or only very weak binding to both of these substrates. At 9.6 nM, the nPfh1-L430V variant had reduced binding to the single-stranded DNA compared to nPfh1 (33% for nPfh1 compared to 26% for nPfh1-L430V) (Figure 5B).

The nPfh1 SM variants cannot displace proteins from DNA but possess strand-annealing activity

We also tested the SM variants for their ability to displace proteins from DNA and to anneal complementary oligonucleotides. None of the variants could displace streptavidin from DNA (Figure 6A), but all of the nPfh1 variants demonstrated strand-annealing activity (Figures 6B and C). Also, annealing of all of the different oligonucleotides was slightly higher for nPfh1-L430V compared to the wild-type nPfh1 and the other SM variants (Figures 3C and 6C). However, the presence of ATP did not have any significant effects on annealing activity. The other SM variants displayed strand-annealing activity that was similar to nPfh1 or slightly higher or slightly lower on the different substrates. These results suggest that the SM does not contribute directly to the strand-annealing activity of nPfh1.

nPfh1 and nPfh1-L430V have similar conformations

Both nPfh1-L430A and nPfh1-L430V were expressed at similar levels as nPfh1 (data not shown), but in the biochemical assays nPfh1-L430V was more similar to wild-type nPfh1 than nPfh1-L430A. The other variants (nPfh1-L430P and nPfh1-Δ21) were produced at lower levels than nPfh1, and their biochemical properties were mostly lower compared to nPfh1, nPfh1-L430A and nPfh1-L430V. We used far-ultraviolet (UV) CD spectroscopy to get an indication of whether the reduction in activity of the less active variants was due to changes in protein conformation. nPfh1 and nPfh1-L430V displayed almost identical CD spectra (Figure 7), which together with their very similar yield of soluble protein and the high enzymatic activity of nPfh1-L430V suggests that nPfh1-L430V has a similar conformation as wild-type nPfh1. For nPfh1-L430A, the collected CD spectrum had a slightly different profile compared to the other two proteins (Figure 7), and lower signal intensity and signal-to-noise ratio. It appears that despite the good expression level and yield of nPfh1-L430A, the secondary structure of the mutant differs slightly from wild-type nPfh1. This change in secondary structure probably reflects conformational alterations and might explain the lower helicase and binding activities of nPfh1-L430A compared to nPfh1 and nPfh1-L430V.

DISCUSSION

As far as we are aware, no other studies that have been performed on either the *in vitro* or *in vivo* functions of the SM in eukaryotes. Here we provide a detailed analysis of the biochemical properties of *S. pombe* nPfh1, including the role of the SM. Our *in vitro* findings complement those in the accompanying paper that mainly focuses on the *in vivo* functions of the ScPif1 SM.

We show that at low protein concentrations (96 pM), nPfh1 was 4.5-fold more efficient at unwinding RNA/DNA substrates compared to DNA/DNA substrates (Figure 1), even though the binding of nPfh1 was similar for both substrates (Figure 2). ScPif1 also has enhanced activity on RNA/DNA substrates (29,30). Together, these findings suggest that Pif1 family helicases might resolve RNA/DNA hybrids such as R-loops. Another important finding was that nPfh1 was able to displace streptavidin from biotinylated DNA (Figure 3A) even though the interaction between streptavidin and biotin is very strong. Similarly, ScPif1 can displace a tightly bound protein from DNA (33–35). This activity provides an appealing explanation for nPfh1's ability to promote fork progression at sites bound by stable non-nucleosomal protein complexes, such as at the replication fork barriers in rDNA and mating type loci (23,26). This activity might also allow nPfh1 to remove the transcription preinitiation complex from tDNA genes and thereby promote fork progression at these genes (23,24). Alternatively, both the unwinding of R-loops and displacement of proteins could be important for replication of these genes.

During DNA replication, the DNA polymerase α /primase complex synthesizes a primer of ~10 nt RNA and ~20 nt DNA on each Okazaki fragment on the lagging strand (50). We tested the binding and unwinding

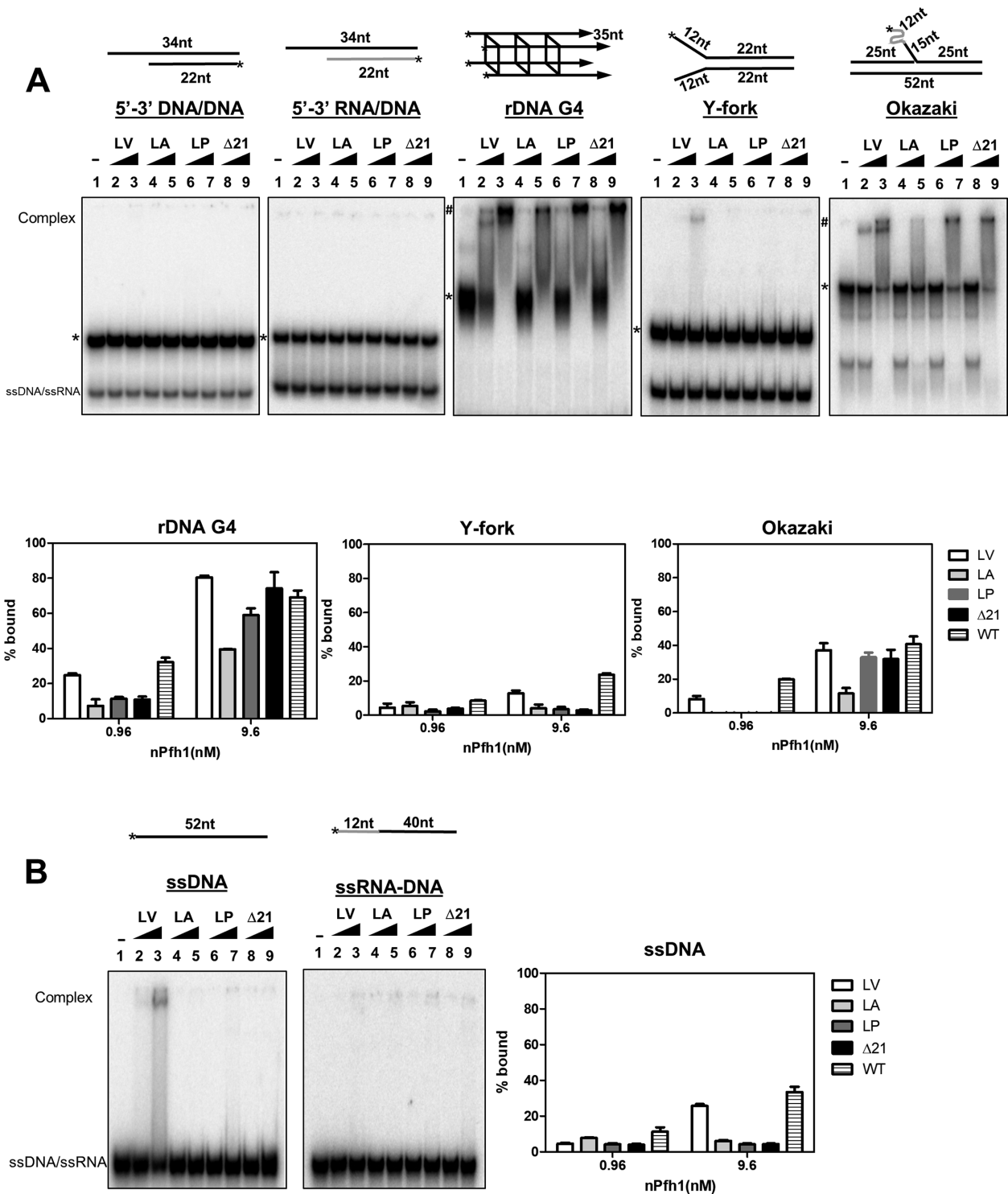


Figure 5. The breast cancer-associated variant nPfh1-L430P in *Schizosaccharomyces pombe* binds G4 DNA and Okazaki fragments (A). (Top) Gel shift assays were conducted as in Figure 2 using either 0.96 or 9.6 nM of the nPfh1 variants LV, LA, LP or Δ21. ‘-’ in lane 1 indicates that protein was not added to the reaction, and ‘*’ indicates the position of the annealed/folded substrate. # indicates protein/DNA in the wells of the rDNA G4 and Okazaki substrates. (Bottom) Graphs showing quantification of three independent gel shift assays for rDNA G4, Y-fork and Okazaki substrates. Quantification data for wild-type nPfh1 are from Figure 2A (B). (Left image) Gel shift assays performed as in (A) with either single-stranded DNA or RNA-DNA oligonucleotides. (Right image) Quantification of the amount of protein bound to single-stranded DNA was calculated from three independent gels.

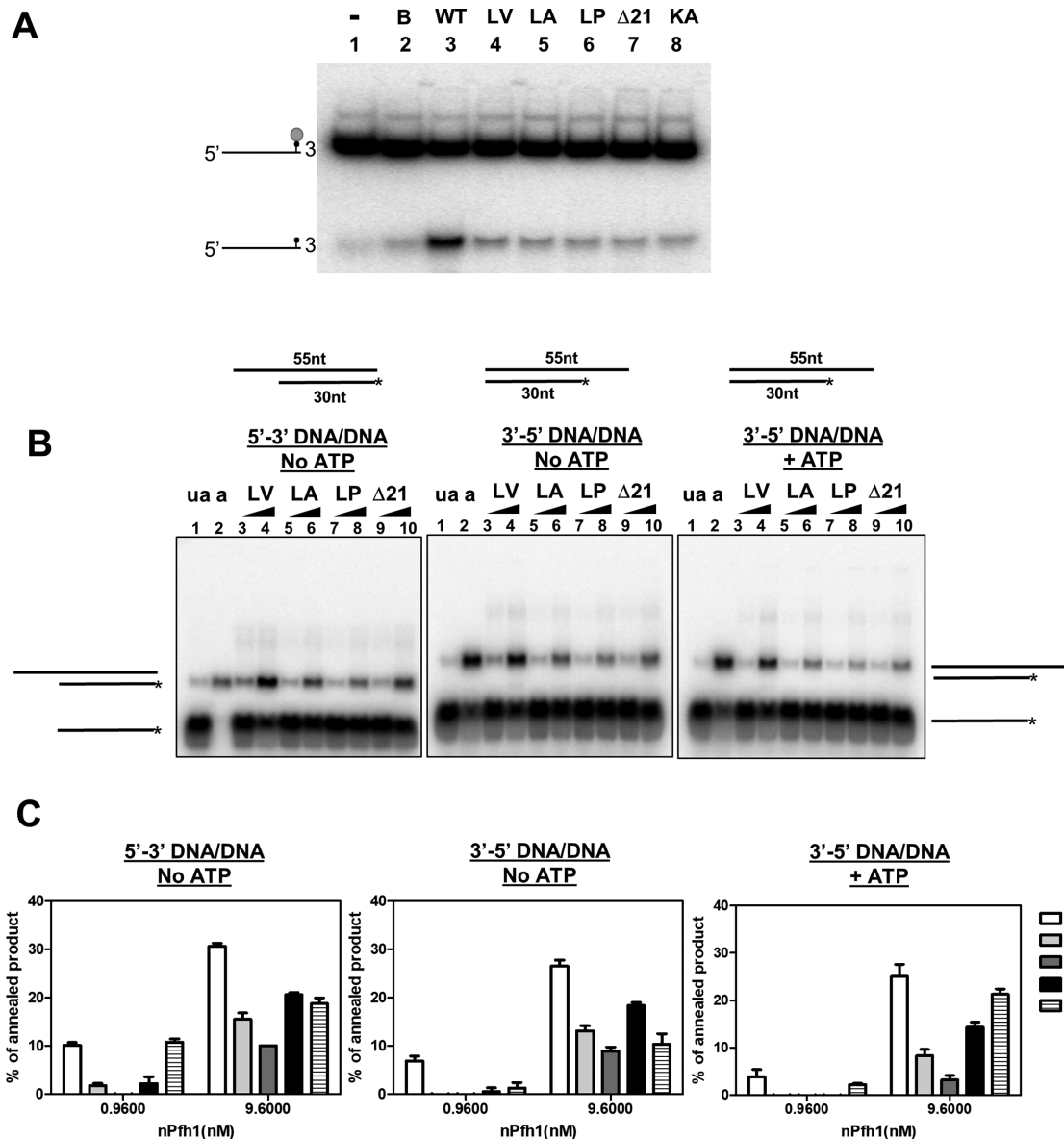


Figure 6. The SM is not required for the strand-annealing activity. (A) A protein displacement assay was conducted as in Figure 3A using either 10 or 25 nM of the WT nPfh1, LV, LA, LP or $\Delta 21$ nPfh1 variants. (B) The strand-annealing experiments were performed as described in Figure 3B with either 0.96 or 9.6 nM of LV, LA, LP or $\Delta 21$ nPfh1. (C) The mean percentage of annealed product was calculated for all four nPfh1 variants. Quantification data for wild-type nPfh1 are from Figure 3B–C.

of nPfh1 to two types of substrates resembling Okazaki fragments. One of the substrates had a 12 nt RNA flap, while the other had a 27 nt RNA–DNA (12 nt RNA and 15 nt DNA) flap. We showed that nPfh1 could bind and unwind both of these substrates (Figures 1 and 2; Supplementary Figure S2); however, both the binding and the unwinding of the Okazaki fragment substrate was much more efficient with the substrate containing the 27 nt flap. This demonstrated that binding and unwinding of nPfh1 is not hindered by ribose in the backbone of the 5' end of the flap and that a longer flap stimulates nPfh1 binding and unwinding. During Okazaki fragment maturation, Pfh1 is suggested to assist Dna2 in processing long flaps that have escaped degradation by flap endonuclease 1 (FEN1)

(28). Our *in vitro* data on nPfh1 support these results and suggest that longer flaps are more suitable substrates than the shorter substrates that FEN1 can process.

In Pif1 helicases, all conserved helicase motifs, including the SM, are present in domains 1A and 2A (40). The SM is folded into an α -helix, a loop and part of a β sheet (41–43). Here we show that SM is essential for both unwinding nucleic acids and protein displacement (Figures 4C and 6A), activities that require ATP hydrolysis. These biochemical functions of Pfh1 SM are consistent with the *in vivo* roles of ScPif1 SM (see accompanying paper by Geronimo *et al.* (39)). For instance, SM of ScPif1 was needed for ScPif1's functions in mtDNA maintenance, and at Okazaki frag-

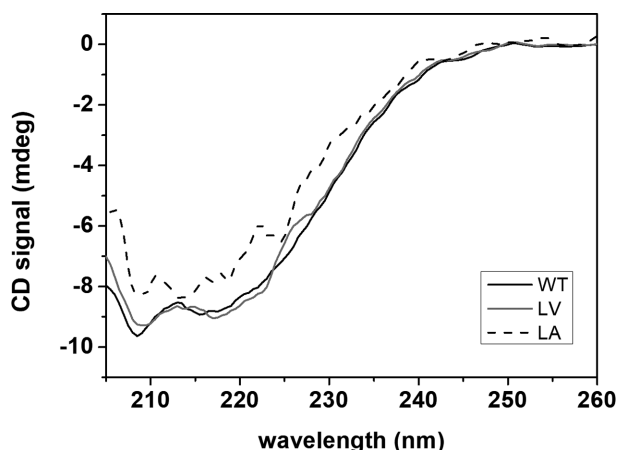


Figure 7. Mutation of leucine to valine in the SM does not change the secondary structure of nPfh1. CD measurements of WT, LV or LA nPfh1 were made between 200 and 260 nm at 30°C.

ment maturation, sites were Pfh1 also act at and most likely in an ATP-dependent manner.

I118 in BaPif1 is located in the SM and corresponds to L430 in *S. pombe* Pfh1, L354 in ScPif1 and L319 in hPIF1 (Figure 4A) (38,41), and the DNA binding and helicase activities of the BaPif1 variants BaPif1-I118A and BaPif1-I118P have been studied *in vitro* (41). BaPif1-I118P does not bind to single-stranded DNA nor does it unwind DNA/DNA partial duplex substrates, while BaPif1-I118A carries out both activities as efficiently as wild-type BaPif1 (41). The crystal structure of BaPif1 shows that I118 interacts with part of the 1A domain, which binds single-stranded DNA (41). It is proposed that a proline at this site, but not an alanine, introduces a kink into the α helix that destabilizes its interaction with the 1A domain (41). Likewise, in the present work nPfh1-L430P was unable to bind single-stranded DNA or to unwind any of the substrates used here (Figures 4 and 5). However, in contrast to the results with BaPif1-I118A, nPfh1-L430A was defective in single-stranded DNA binding, DNA unwinding (6–74-fold lower than nPfh1) and ATP hydrolysis, while nPfh1-L430V was almost as active as wild-type nPfh1 (1.5–3-fold lower unwinding than nPfh1). *In vivo*, ScPif1-L354A shows wild-type ScPif1 properties, suggesting that substituting a leucine to an alanine does not affect the function of ScPif1 in the cell (see accompanying paper by Geronimo *et al.* (39)). Without a Pfh1 structure, it is difficult to explain the discrepancy between the data on nPfh1-L430A compared to BaPif1-I118A, and ScPif1-L354A (see accompanying paper by Geronimo *et al.* (39)), and why nPfh1-L430V has higher activity than nPfh1-L430A. However, we speculate that nPfh1-L430A loses interactions with the 1A domain, which is important for efficient binding to single-stranded DNA. Perhaps the larger side chain of valine compared to alanine is more similar to the leucine side chain and therefore is better at facilitating the interaction with the 1A domain. Remarkably, although both BaPif1-I118P and nPfh1-L430P were unable to bind single-stranded DNA, nPfh1-L430P and all the other nPfh1 variants, including nPfh1- Δ 21, created a DNA shift with the G4 DNA and Okazaki

fragments with long flaps (Figure 5A), suggesting that these variants bind to these substrates. Similarly, the SM was dispensable for binding of recombinant ScPif1 to a structured substrate (see accompanying paper by Geronimo *et al.* (39)). This suggests that the binding of nPfh1 and ScPif1 to some substrates is independent of the SM. Notably, the detected DNA–protein shift with the nPfh1-L430A, nPfh1-L430P and nPfh1- Δ 21 did not migrate into the gel, as it did for wild-type nPfh1, nPfh1-KA and nPfh1-L430V. This slower migrating complex was detected for wild-type nPfh1, nPfh1-KA and nPfh1-L430V only at high protein concentrations (Figures 2A and 5A) and suggests that the nPfh1-L430A, nPfh1-L430P and nPfh1- Δ 21 variants do not bind these substrates as monomers, but maybe as dimers or other multimers. This suggests that the SM is important for the binding of the monomeric form of nPfh1, but dispensable for multimeric forms of nPfh1 to some substrates.

We also demonstrated that nPfh1 has an ATP-independent strand-annealing activity, an activity also seen in hPIF1 and ScPif1 (36,46). The SM was dispensable for nPfh1's strand-annealing activity (Figure 6B), and some of the SM variants showed even higher strand-annealing activity than wild-type nPfh1. Several other helicase families carry out strand-annealing *in vitro* (45). For example, the Bloom syndrome (BLM) helicase, whose mutation causes the cancer-prone Bloom's syndrome, has helicase and annealing activities. As we show for nPfh1-L430P, the missense mutation C878R in BLM, which is also linked to cancer, shows no unwinding activity but possesses strand-annealing activity (51). Together, these data suggest that proper regulation of the unwinding and annealing activities is important for preserving genome stability.

How helicases coordinate their unwinding and rewinding activities is not known. One suggestion is that ATP binding triggers a conformational change that inhibits strand-annealing and promotes unwinding (45). However, in our experiments, ATP had the opposite effect on nPfh1, as it stimulated its strand-annealing activity. The *in vivo* importance of the annealing activity has not been determined for any helicase, and identifying a mutation that eliminates this activity *in vitro* in a genetically tractable organism like *S. pombe* might help establish its *in vivo* role.

In this study, we have identified several new activities for nPfh1. We found that nPfh1 preferably unwinds RNA/DNA compared to DNA/DNA substrates, it displaces proteins from DNA, and it possesses a strand-annealing activity. The binding preference of nPfh1 for different substrates agrees well with nPfh1's unwinding efficiency, and the top four substrates were rDNA G4 > Okazaki fragment substrate with 27 nt flap > Y-fork > RNA/DNA partial duplex. We also demonstrated that the SM is essential for all of nPfh1's *in vitro* activities, except strand-annealing, and for binding to some DNA substrates, suggesting that the SM is essential for activities that require ATP, but dispensable for binding to some substrates. The SM of ScPif1 was required for ATP-dependent *in vivo* and *in vitro* functions (see accompanying paper by Geronimo *et al.* (39)). Therefore, the work in these two papers suggest that the SM in Pif1 helicases involves activities that require ATP binding or hydrolysis (see accompanying paper by Geronimo *et al.* (39)).

Finally, if the cancer-associated hPIF1 variant can bind and rewind nucleic acids, but not unwind them, this would raise the possibility that binding without unwinding might be the pathological explanation for the genome integrity defects of the cancer-associated allele.

SUPPLEMENTARY DATA

Supplementary Data are available at NAR Online.

ACKNOWLEDGEMENTS

We thank Gunter Stier (Universität Heidelberg, Germany) for providing us with the modified pET-22b vectors.

FUNDING

Swedish Research Council; Swedish Society for Medical Research; Insamlingsstiftelsen at Umeå University; Knut and Alice Wallenberg Foundations. Funding for open access charge: Knut och Alice Wallenbergs Stiftelse.

Conflict of interest statement. None declared.

REFERENCES

- Bochman, M.L., Sabouri, N. and Zakian, V.A. (2010) Unwinding the functions of the Pif1 family helicases. *DNA Repair*, **9**, 237–249.
- Bochman, M.L., Judge, C.P. and Zakian, V.A. (2011) The Pif1 family in prokaryotes: what are our helicases doing in your bacteria? *Mol. Biol. Cell*, **22**, 1955–1959.
- Osmundson, J.S., Kumar, J., Yeung, R. and Smith, D.J. (2017) Pif1-family helicases cooperatively suppress widespread replication-fork arrest at tRNA genes. *Nature Struct. Mol. Biol.* **24**, 162–170.
- Zhou, J., Monson, E.K., Teng, S.C., Schulz, V.P. and Zakian, V.A. (2000) Pif1p helicase, a catalytic inhibitor of telomerase in yeast. *Science*, **289**, 771–774.
- Boule, J.B., Vega, L.R. and Zakian, V.A. (2005) The yeast Pif1p helicase removes telomerase from telomeric DNA. *Nature*, **438**, 57–61.
- Saini, N., Ramakrishnan, S., Elango, R., Ayyar, S., Zhang, Y., Deem, A., Ira, G., Haber, J.E., Lobachev, K.S. and Malkova, A. (2013) Migrating bubble during break-induced replication drives conservative DNA synthesis. *Nature*, **502**, 389–392.
- Wilson, M.A., Kwon, Y., Xu, Y., Chung, W.H., Chi, P., Niu, H., Mayle, R., Chen, X., Malkova, A., Sung, P. et al. (2013) Pif1 helicase and Poldelta promote recombination-coupled DNA synthesis via bubble migration. *Nature*, **502**, 393–396.
- Budd, M.E., Reis, C.C., Smith, S., Myung, K. and Campbell, J.L. (2006) Evidence suggesting that Pif1 helicase functions in DNA replication with the Dna2 helicase/nuclease and DNA polymerase delta. *Mol. Cell Biol.* **26**, 2490–2500.
- Pike, J.E., Burgers, P.M., Campbell, J.L. and Bambara, R.A. (2009) Pif1 helicase lengthens some Okazaki fragment flaps necessitating Dna2 nuclease/helicase action in the two-nuclease processing pathway. *J. Biol. Chem.* **284**, 25170–25180.
- Schulz, V.P. and Zakian, V.A. (1994) The saccharomyces PIF1 DNA helicase inhibits telomere elongation and de novo telomere formation. *Cell*, **76**, 145–155.
- Lahaye, A., Leterme, S. and Foury, F. (1993) PIF1 DNA helicase from *Saccharomyces cerevisiae*. Biochemical characterization of the enzyme. *J. Biol. Chem.* **268**, 26155–26161.
- Foury, F. and Kolodnynski, J. (1983) pif mutation blocks recombination between mitochondrial rho+ and rho- genomes having tandemly arrayed repeat units in *Saccharomyces cerevisiae*. *Proc. Natl. Acad. Sci. U.S.A.*, **80**, 5345–5349.
- Ivessa, A.S., Zhou, J.Q. and Zakian, V.A. (2000) The *Saccharomyces* Pif1p DNA helicase and the highly related Rrm3p have opposite effects on replication fork progression in ribosomal DNA. *Cell*, **100**, 479–489.
- Ivessa, A.S., Zhou, J.Q., Schulz, V.P., Monson, E.K. and Zakian, V.A. (2002) *Saccharomyces* Rrm3p, a 5' to 3' DNA helicase that promotes replication fork progression through telomeric and subtelomeric DNA. *Genes Dev.* **16**, 1383–1396.
- Ivessa, A.S., Lenzmeier, B.A., Bessler, J.B., Goudsouzian, L.K., Schnakenberg, S.L. and Zakian, V.A. (2003) The *Saccharomyces cerevisiae* helicase Rrm3p facilitates replication past nonhistone protein-DNA complexes. *Mol. Cell*, **12**, 1525–1536.
- Azvolinsky, A., Dunaway, S., Torres, J.Z., Bessler, J.B. and Zakian, V.A. (2006) The *S. cerevisiae* Rrm3p DNA helicase moves with the replication fork and affects replication of all yeast chromosomes. *Genes Dev.* **20**, 3104–3116.
- Tran, P.L.T., Pohl, T.J., Chen, C.F., Chan, A., Pott, S. and Zakian, V.A. (2017) PIF1 family DNA helicases suppress R-loop mediated genome instability at tRNA genes. *Nature Commun.* **8**, 15025.
- Paeschke, K., Bochman, M.L., Garcia, P.D., Cejka, P., Friedman, K.L., Kowalczykowski, S.C. and Zakian, V.A. (2013) Pif1 family helicases suppress genome instability at G-quadruplex motifs. *Nature*, **497**, 458–462.
- Paeschke, K., Capra, J.A. and Zakian, V.A. (2011) DNA replication through G-quadruplex motifs is promoted by the *Saccharomyces cerevisiae* Pif1 DNA helicase. *Cell*, **145**, 678–691.
- Sabouri, N. (2017) The functions of the multi-tasking Pfh1 (Pif1) helicase. *Curr. Genet.* **63**, 621–626.
- Pinter, S.F., Aubert, S.D. and Zakian, V.A. (2008) The *Schizosaccharomyces pombe* Pfh1p DNA helicase is essential for the maintenance of nuclear and mitochondrial DNA. *Mol. Cell Biol.* **28**, 6594–6608.
- McDonald, K.R., Guise, A.J., Pourbozorgi-Langroudi, P., Cristea, I.M., Zakian, V.A., Capra, J.A. and Sabouri, N. (2016) Pfh1 is an accessory replicative helicase that interacts with the replisome to facilitate fork progression and preserve genome integrity. *PLoS Genet.* **12**, e1006238.
- Sabouri, N., McDonald, K.R., Webb, C.J., Cristea, I.M. and Zakian, V.A. (2012) DNA replication through hard-to-replicate sites, including both highly transcribed RNA Pol II and Pol III genes, requires the *S. pombe* Pfh1 helicase. *Genes Dev.* **26**, 581–593.
- McDonald, K.R., Sabouri, N., Webb, C.J. and Zakian, V.A. (2014) The Pif1 family helicase Pfh1 facilitates telomere replication and has an RPA-dependent role during telomere lengthening. *DNA Repair*, **24**, 80–86.
- Sabouri, N., Capra, J.A. and Zakian, V.A. (2014) The essential *Schizosaccharomyces pombe* Pfh1 DNA helicase promotes fork movement past G-quadruplex motifs to prevent DNA damage. *BMC Biol.* **12**, 101.
- Steinacher, R., Osman, F., Dalgaard, J.Z., Lorenz, A. and Whitby, M.C. (2012) The DNA helicase Pfh1 promotes fork merging at replication termination sites to ensure genome stability. *Genes Dev.* **26**, 594–602.
- Azvolinsky, A., Giresi, P.G., Lieb, J.D. and Zakian, V.A. (2009) Highly transcribed RNA polymerase II genes are impediments to replication fork progression in *Saccharomyces cerevisiae*. *Mol. Cell*, **34**, 722–734.
- Ryu, G.H., Tanaka, H., Kim, D.H., Kim, J.H., Bae, S.H., Kwon, Y.N., Rhee, J.S., MacNeill, S.A. and Seo, Y.S. (2004) Genetic and biochemical analyses of Pfh1 DNA helicase function in fission yeast. *Nucleic Acids Res.* **32**, 4205–4216.
- Chib, S., Byrd, A.K. and Raney, K.D. (2016) Yeast Helicase Pif1 unwinds RNA:DNA hybrids with higher processivity than DNA:DNA duplexes. *J. Biol. Chem.* **291**, 5889–5901.
- Boule, J.B. and Zakian, V.A. (2007) The yeast Pif1p DNA helicase preferentially unwinds RNA DNA substrates. *Nucleic Acids Res.* **35**, 5809–5818.
- Byrd, A.K. and Raney, K.D. (2015) A parallel quadruplex DNA is bound tightly but unfolded slowly by pif1 helicase. *J. Biol. Chem.* **290**, 6482–6494.
- Zhou, R., Zhang, J., Bochman, M.L., Zakian, V.A. and Ha, T. (2014) Periodic DNA patrolling underlies diverse functions of Pif1 on R-loops and G-rich DNA. *eLife*, **3**, e02190.
- Koc, K.N., Singh, S.P., Stodola, J.L., Burgers, P.M. and Galletto, R. (2016) Pif1 removes a Rap1-dependent barrier to the strand displacement activity of DNA polymerase delta. *Nucleic Acids Res.* **44**, 3811–3819.

34. Galletto,R. and Tomko,E.J. (2013) Translocation of *Saccharomyces cerevisiae* Pif1 helicase monomers on single-stranded DNA. *Nucleic Acids Res.*, **41**, 4613–4627.
35. Ramanagoudr-Bhojappa,R., Chib,S., Byrd,A.K., Aarattuthodiyil,S., Pandey,M., Patel,S.S. and Raney,K.D. (2013) Yeast Pif1 helicase exhibits a one-base-pair stepping mechanism for unwinding duplex DNA. *J. Biol. Chem.*, **288**, 16185–16195.
36. Ramanagoudr-Bhojappa,R., Byrd,A.K., Dahl,C. and Raney,K.D. (2014) Yeast Pif1 accelerates annealing of complementary DNA strands. *Biochemistry*, **53**, 7659–7669.
37. Wallgren,M., Mohammad,J.B., Yan,K.P., Pourbozorgi-Langroudi,P., Ebrahimi,M. and Sabouri,N. (2016) G-rich telomeric and ribosomal DNA sequences from the fission yeast genome form stable G-quadruplex DNA structures in vitro and are unwound by the Pfh1 DNA helicase. *Nucleic Acids Res.*, **44**, 6213–6231.
38. Chisholm,K.M., Aubert,S.D., Freese,K.P., Zakian,V.A., King,M.C. and Welch,P.L. (2012) A genomewide screen for suppressors of Alu-mediated rearrangements reveals a role for PIF1. *PLoS One*, **7**, e30748.
39. Geronimo,C.L., Singh,S.P., Galletto,R and Zakian,V.A. (2018) Thesignature motif of the *Saccharomyces cerevisiae* Pif1 DNA helicase is essential *in vivo* for mitochondrial and nuclear functions and *in vitro* for ATPase activity. *Nucleic Acids Res.*, doi:10.1093/nar/gky655.
40. Byrd,A.K. and Raney,K.D. (2017) Structure and function of Pif1 helicase. *Biochem. Soc. Trans.*, **45**, 1159–1171.
41. Zhou,X., Ren,W., Bharath,S.R., Tang,X., He,Y., Chen,C., Liu,Z., Li,D. and Song,H. (2016) Structural and functional insights into the unwinding mechanism of bacteroides sp Pif1. *Cell Rep.*, **14**, 2030–2039.
42. Chen,W.F., Dai,Y.X., Duan,X.L., Liu,N.N., Shi,W., Li,N., Li,M., Dou,S.X., Dong,Y.H., Rety,S. *et al.* (2016) Crystal structures of the BsPif1 helicase reveal that a major movement of the 2B SH3 domain is required for DNA unwinding. *Nucleic Acids Res.*, **44**, 2949–2961.
43. Lu,K.Y., Chen,W.F., Rety,S., Liu,N.N., Wu,W.Q., Dai,Y.X., Li,D., Ma,H.Y., Dou,S.X. and Xi,X.G. (2017) Insights into the structural and mechanistic basis of multifunctional *S. cerevisiae* Pif1p helicase. *Nucleic Acids Res.*, **46**, 1486–1500.
44. Bruning,J.G., Howard,J.A. and McGlynn,P. (2016) Use of streptavidin bound to biotinylated DNA structures as model substrates for analysis of nucleoprotein complex disruption by helicases. *Methods*, **108**, 48–55.
45. Wu,Y. (2012) Unwinding and rewinding: double faces of helicase? *J. Nucleic Acids*, **2012**, 140601.
46. Gu,Y., Masuda,Y. and Kamiya,K. (2008) Biochemical analysis of human PIF1 helicase and functions of its N-terminal domain. *Nucleic Acids Res.*, **36**, 6295–6308.
47. Goujon,M., McWilliam,H., Li,W., Valentin,F., Squizzato,S., Paern,J. and Lopez,R. (2010) A new bioinformatics analysis tools framework at EMBL-EBI. *Nucleic Acids Res.*, **38**, W695–W699.
48. Wood,V., Gwilliam,R., Rajandream,M.A., Lyne,M., Lyne,R., Stewart,A., Sgouros,J., Peat,N., Hayles,J., Baker,S. *et al.* (2002) The genome sequence of *Schizosaccharomyces pombe*. *Nature*, **415**, 871–880.
49. Okonechnikov,K., Golosova,O., Fursov,M. and Team,U. (2012) Unipro UGENE: a unified bioinformatics toolkit. *Bioinformatics*, **28**, 1166–1167.
50. Burgers,P.M.J. and Kunkel,T.A. (2017) Eukaryotic DNA replication fork. *Annu. Rev. Biochem.*, **86**, 417–438.
51. Guo,R.B., Rigolet,P., Ren,H., Zhang,B., Zhang,X.D., Dou,S.X., Wang,P.Y., Amor-Gueret,M. and Xi,X.G. (2007) Structural and functional analyses of disease-causing missense mutations in Bloom syndrome protein. *Nucleic Acids Res.*, **35**, 6297–6310.